Acoustical coupling in self-oscillating computational vocal fold models

Scott Thomson

Acoustical coupling in self-oscillating computational vocal fold models

S. L. Thomson

1) Brigham Young University, 2) University Erlangen-Nuremberg, 435 CTB, Provo, 84602, USA
thomson@byu.edu

Synthetic vocal fold models with either one layer or two layers of differing stiffness have been used to study vocal fold vibration. It has been demonstrated, however, that apparently unlike the human vocal folds, these models exhibit strong acoustic coupling with their subglottic flow supply tubes. A synthetic vocal fold model has been recently developed that may not exhibit this acoustic coupling. The model includes four layers of different silicone materials, including epithelial and very flexible superficial lamina propria (SLLP) layers. Its vibratory motion is similar to that of the human vocal folds. To study the degree to which this type of model is acoustically-coupled, finite element models with coupled fluid and solid domains were developed to simulate flow-induced vibration responses. The solid domain included layers corresponding to the four synthetic model layers and allowed for large strain and stress. The fluid domain was governed by the slightly-compressible Navier-Stokes equations, allowing for exploration of acoustic coupling. For comparison, two-layer models were also studied. The results show the two-layer models required acoustic coupling for self-sustained oscillation, whereas the four-layer models did not.

1 Introduction

Vocal fold oscillation is a consequence of flow-structure-acoustic interaction within the human larynx and respiratory airway. To initiate typical voicing, vocal folds are adducted and lung pressure is increased, resulting in vocal fold flow-induced vibration. A periodic jet is formed in the vocal tract, the accompanying pressure fluctuations of which are the primary sound source in voiced speech.

Synthetic and computational models are useful tools for studying the vibration, aerodynamics, and acoustics of voice production. Synthetic vocal fold models such as the so-called "one-layer" [1] and "two-layer" [2] models have been shown to exhibit favorable similarities with human vocal fold vibration. These models consist of one or two layers of flexible silicone materials. In the two-layer model, the silicone materials are of different stiffness, mimicking the body-cover description of human vocal fold tissue [3] in which the cover is more flexible than the body.

Typically these models vibrate at pressures, frequencies, and amplitudes typical of the human vocal folds [1,2]. However, the models have been shown to exhibit two major disadvantages. First, their vibration patterns lack evidence of mucosal wave-like motion [2], a quality that is important in healthy human vocal fold vibration. Second, several of these models have been shown to exhibit acoustic coupling with subglottic flow supply tubes. Two ways that this acoustic coupling has been manifest include: (1) the models synchronize with subglottic resonant frequencies, and (2) the models vibrate only when used with subglottic ducts that are longer than what is physiologically realistic, unless the models are sufficiently flexible [4-7].

A recently-developed synthetic vocal fold model has shown promise in overcoming these two disadvantages. This model has four layers to more closely represent the multi-layer human vocal fold tissue composition, including epithelium, superficial lamina propria, ligament, and muscle layers.

This model has been shown to vibrate with mucosal wave-like motion [8,9]. It has been speculated that it also exhibits reduced subglottic acoustic coupling, although this has yet to be confirmed. Consequently, the research described in this paper was undertaken to explore this issue. Computational two- and four-layer self-oscillating finite element models were developed. Their flow-induced responses with different lengths of subglottic ducts were simulated. In the following sections the numerical methods are summarized and the simulated responses are presented and discussed. Using measures of frequency and subglottic pressure, conclusions are drawn regarding the nature of the acoustic coupling of the four-layer model.

2 Computational Methods

2.1 Fluid domain

The computational models included distinct but fully-coupled two-dimensional fluid and solid domains. The fluid domain (Figure 1) consisted of between approximately 40000 and 63000 1st-order elements and nodes (depending on subglottic length). Dimensions and boundary conditions are given in Tables 1 and 2, respectively. The flow was modeled using the two-dimensional Navier-Stokes equations with assumptions of unsteady, viscous, slightly compressible flow [10]. The fluid was air with a density of 1.2 kg/m^3, a viscosity of 1.8×10^{-5} Pa·s, and a bulk modulus of 1.41×10^5 Pa. Time marching was performed using a 2nd-order composite scheme with a time step size of 25×10^{-6} s.

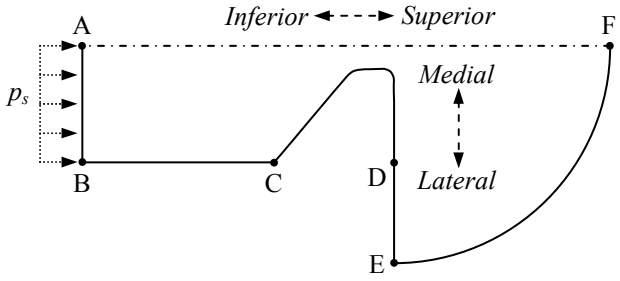

Figure 1: One half of the fluid domain along with anatomical orientations (not to scale). Geometry was initially symmetric about the centerline (AF).

Table 1: Fluid domain coordinates. *L* denotes the subglottic duct length and varied from 5 to 50 cm.

Point	*x* (cm)	*y* (cm)
A	−*L*	0
B	−*L*	−0.845
C	0	−0.845
D	1.075	−0.845
E	1.075	−50
F	51.075	0

Table 2: Fluid domain boundary conditions.

Section	Boundary Condition
Line AB	Constant pressure (900 Pa)
Line BC	Wall
Line CD	Fluid-structure interface
Line DE	Wall
Arc EF	Zero pressure

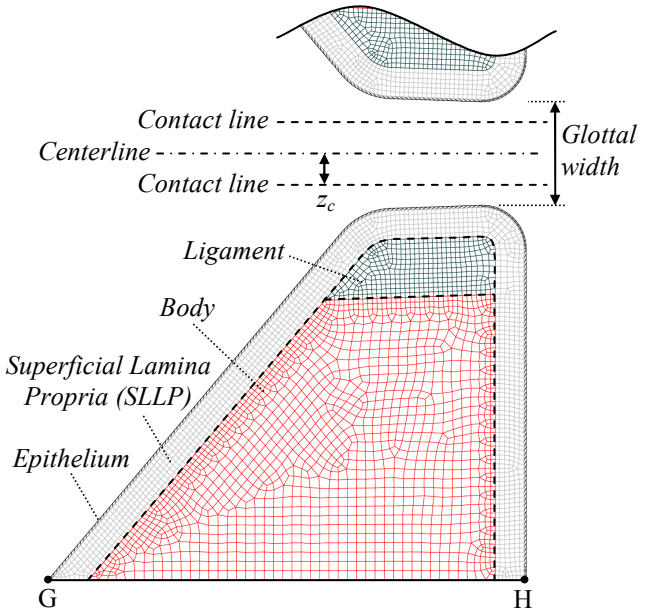

Figure 2: Solid domain geometry (glottal gap not to scale).

2.2 Solid domain

The solid domain consisted of two vocal fold models, one of which is shown in Figure 2, and consisted of approximately 6500 second-order elements with 27000 nodes. Complete geometry definitions and values can be found in [11]; a few values are here provided for reference: the distance between points G and H was 1.07 cm, the epithelium layer was 50 μm thick, and the SLLP layer was 0.65 mm thick. The solid solver allowed for large deformation and strain. The solid domain was coupled with the fluid domain by means of a fluid-structure interaction boundary condition along the exterior of the epithelium. This boundary condition enforced consistent solid and fluid domain stress and displacement along the wetted interface. Displacement and rotation values along line GH were constrained to be zero. The initial glottal width was 100 μm. In the solid domain, two contact lines were used to prevent complete collapse of the fluid mesh as the vocal folds approached each other. The lines were midway between each vocal fold and the centerline (z_c = 25 μm), resulting in a minimum gap during glottal closure of 50 μm.

2.3 Cases

Four different models were studied: two two-layer models and two four-layer models. The response of each model was simulated using three different duct lengths: 5, 20, and 50 cm. The cases are here denoted by the following character sequence: first, the number of layers (2 or 4), second, a letter label for the stiffness subset (A or B, described below), and third, the length of the duct in cm. For example, case 4B20 denotes the simulation of the 4B model with a duct length of 20 cm.

All model layers were defined using a Poisson's ratio of 0.49 and a density of 1070 kg/m^3. The two-layer model stiffness sets (2A and 2B) were materially-linear with Young's modulus values as shown in the Table 3. (Note that while four layers are listed in Table 3, models 2A and 2B had two effective layers by using matching Young's modulus values.) The Young's modulus values of model 2B were twice those of model 2A.

The epithelium of models 4A and 4B was also materially linear, defined with a Young's modulus of 50 kPa. The other three layers were defined using the stress-strain relation $\sigma(\varepsilon) = F(e^{10.5\varepsilon} - 1)$, where σ is stress, F is a layer-specific parameter, and ε is strain. F was 112.7 and 1408.5 for the ligament and body layers, respectively, of models 4A and 4B. Values of F = 22.54 and F = 45.07 were assigned to the SLLP layers of models 4A and 4B, respectively. At 5% strain these values of F yielded the tangent modulus values shown in Table 3 for the three materially-nonlinear layers of models 4A and 4B. The SLLP stiffness of model 4B was twice that of model 4A. Because of the exceeding flexibility of the SLLP layers of both four-layer models (much more flexible than the cover of the two-layer models, the cover being the combined epithelium and SLLP layers), the epithelial layer was required to help "encapsulate" the SLLP layer.

Table 3: Solid domain modulus values for two- and four-layer models. ML stands for "materially linear."

Model	Epithelium	SLLP	Ligament	Body
2A	5 kPa (ML)	5 kPa (ML)	15 kPa (ML)	15 kPa (ML)
2B	10 kPa (ML)	10 kPa (ML)	30 kPa (ML)	30 kPa (ML)
4A	50 kPa (ML)	0.4 kPa	2 kPa	25 kPa
4B	50 kPa (ML)	0.8 kPa	2 kPa	25 kPa

3 Results

3.1 Two-layer model response

The two-layer models did not vibrate with L = 5 or 20 cm, but did vibrate with L = 50 cm. This can be seen by the glottal width waveforms from cases 2A5, 2A20, and 2A50 shown in Figure 3 (glottal width is the minimum distance between the vocal folds, see Figure 2). Cases 2A5 and 2A20 experienced a transient vibration that decayed by 100 ms. By contrast, case 2A50 showed self-sustained oscillation with a maximum glottal width of approximately 1.1 mm and a frequency of 136 Hz. These glottal width and frequency values are comparable to human values [12,13].

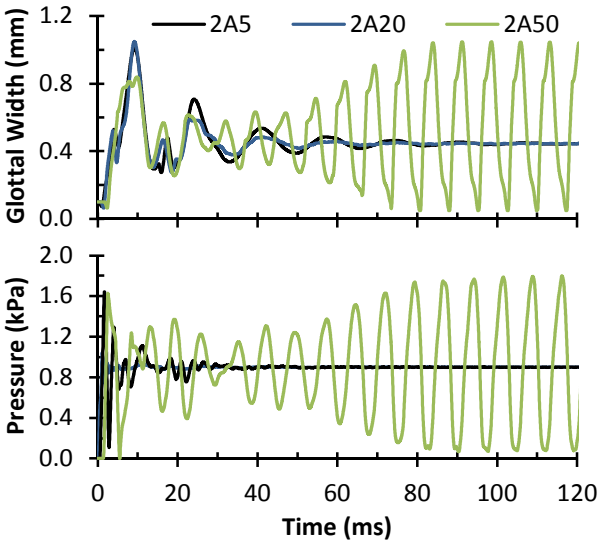

Figure 3: Glottal width and pressure waveforms predicted by two-layer model cases 2A5, 2A20, and 2A50.

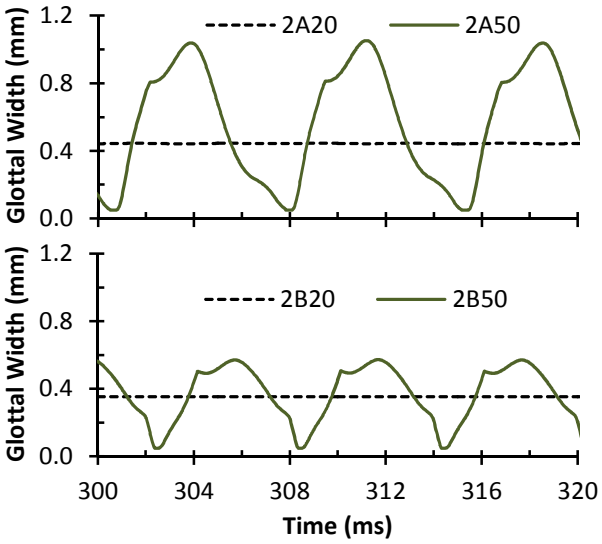

Figure 4: Steady-state glottal width waveforms for two-layer model cases 2A50 (top) and 2B50 (bottom).

The corresponding pressure waveforms are also shown in Figure 3. The non-self-oscillating cases reached a steady value of 900 Pa (the inlet pressure), whereas during steady-state oscillation, the self-oscillating case pressure waveform fluctuated between approximately 77 Pa and 1770 Pa with a mean of 903 Pa.

The 2B cases responded similarly in that self-sustained oscillation was only achieved for the 50 cm duct. However, the frequency was higher (167 Hz) and the maximum glottal width was lower (0.57 mm) (see Figure 4).

3.2 Four-layer model response

In contrast with the two-layer models, the four-layer models self-oscillated at all duct lengths (see Figure 5 for 4A model steady-state responses). The maximum glottal width values were 0.79, 1.15, and 1.05 mm for the 4A5, 4A20, and 4A50 cases, respectively. The respective frequencies were 220, 260, and 203 Hz, which is near the range of the female voice. Considerable difference is also seen between the waveforms of the three cases.

The 4B5 and 4B20 cases yielded similar predictions as the corresponding 4A cases, only with slightly lower amplitude (the 4B50 case failed due to severe mesh deformation). Whereas the 2B50 case vibrated at a much higher frequency than the 2A50 case, the 4B cases yielded nearly the same frequencies as their 4A counterparts.

4 Discussion

The two-layer model required subglottic coupling for vibration as evidenced by the lack of vibration of the two-layer model with duct lengths less than 50 cm. This is consistent with the experimental results of Zhang et al. [4] in which one-layer model vibration was found to only be sustained with duct lengths greater than 30 cm. Regarding the four-layer models, it is clear that subglottic coupling was not required for self-oscillation. However, this should not be interpreted to mean that the model vibration was independent of subglottic influences.

To examine these results it is helpful to compare the flow-induced vibration frequencies with estimates of the duct resonance frequencies and modal vibration frequencies. The modal vibrations are listed in Table 4. Treating the duct as a closed duct, the resonance frequencies can be estimated as $f_n = nc/(4L)$, where f_n is the frequency (Hz) associated with the n^{th} harmonic (n = 1, 3, 5, …), c is the speed of sound in air (here 343 m/s), and L is the duct length. This equation yields fundamental frequencies of 1715, 429, and 172 Hz for duct lengths of L = 0.05, 0.2, and 0.5 m, respectively.

Table 4: Modal frequencies (Hz) for the four cases.

Model	f_1	f_2	f_3	f_4	f_5	f_6
2A	60.2	129	151	233	261	293
2B	85.1	182	214	329	370	414
4A	61.4	115	124	142	159	175
4B	63.0	121	136	166	183	206

The 2A and 2B modal vibration frequencies were all significantly lower than the fundamental resonance frequencies of the two shorter ducts, but in the range of the longer duct's resonant frequency. This suggests that the 2A and 2B models coupled with the resonant frequencies of the longer duct to achieve flow-induced vibration. This has been termed an "acoustically-driven" mode of vibration [5,6]. The flow-induced frequency of the 2B case was higher than that of the 2A case. This is attributed to the significantly stiffer 2B material property. It is therefore evident that the 2B model did not necessarily lock into the above-estimated ¼-wavelength duct resonant frequency. This is not surprising given that the estimate was based on a rigid termination, whereas the model stiffness directly influenced the termination stiffness.

The high frequency pressure oscillations of case 4A5 in Figure 5 have a frequency of approximately 1740 Hz and the higher frequency pressure oscillations of case 4A20 in Figure 5 have a frequency of approximately 520 Hz. While these are comparable to the fundamental resonance

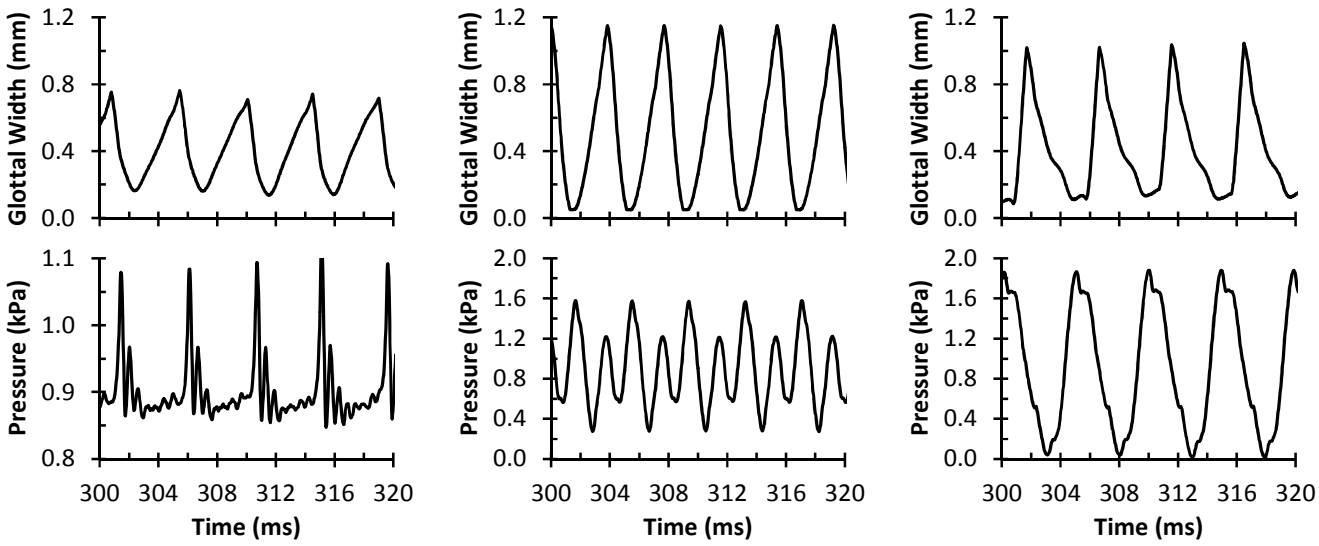

Figure 5: Four-layer model glottal width (top row) and pressure (bottom) waveforms for cases 4A5 (left), 4A20 (middle), and 4A50 (right). For visibility the pressure axis for case 4A5 is different than for the other two cases.

frequencies of the respective ducts, the model vibration frequency was much lower.

5 Conclusion

These simulations of two- and four-layer computational vocal fold model self-oscillations provide evidence that coupling with the subglottic duct is essential for self-sustained vibration of stiff two-layer, but not the present four-layer, models. Based in part on the experimental observation of Zhang et al. [6] that two-layer models with sufficiently soft cover layers vibrated at shorter duct lengths – thus apparently without acoustic coupling – than two-layer models with stiffer cover layers, the reduced acoustical coupling in the four-layer model is attributed to the exceedingly flexible SLLP layer. The human vocal folds likely do not require subglottic coupling. These results, combined with those of Murray and Thomson [9] showing that similar four-layer models yield reasonably life-like mucosal wave-like motion, lead to the conclusion that the four-layer model is a better analog of the human vocal folds than the two-layer model.

Acknowledgments

This project was supported by Award Number R01DC009616 from the National Institute on Deafness and Other Communication Disorders (NIDCD). Its content is solely the responsibility of the authors and does not necessarily represent the official views of the NIDCD or the National Institutes of Health. Sabbatical support of SLT from the University of Erlangen-Nürnberg Graduate School in Advanced Optical Technologies (SAOT) is gratefully acknowledged.

References

[1] S.L. Thomson, L. Mongeau, S.H. Frankel, "Aerodynamic transfer of energy to the vocal folds," *J. Acoust. Soc. Am.* 118(3), 1689-1700 (2005)

[2] J.S. Drechsel, S.L. Thomson, "Influence of supraglottal structures on the glottal jet exiting a two-layer synthetic, self-oscillating vocal fold model," *J. Acoust. Soc. Am.* 123(6), 4434-4445 (2008).

[3] M. Hirano, Y. Kakita, "Cover-body theory of vocal fold vibration", *Speech Science: Recent Advances*, College-Hill Press, San Diego, 1-46 (1985).

[4] Z. Zhang, J. Neubauer, D.A. Berry, "The influence of subglottal acoustics on laboratory models of phonation," *J. Acoust. Soc. Am.* 120(3), 1558-1569 (2006)

[5] Z. Zhang, J. Neubauer, D.A. Berry, "Aerodynamically and acoustically driven modes of vibration in a physical model of the vocal folds," *J. Acoust. Soc. Am.* 120(5), 2841-2849 (2006)

[6] Z. Zhang, J. Neubauer, D.A. Berry, "Influence of vocal fold stiffness and acoustic loading on flow-induced vibration of a single-layer vocal fold model," *J. Sound Vib.* 322, 299-313 (2009)

[7] J.S. Drechsel. *Characterization of Synthetic, Self-Oscillating Vocal Fold Models*. MS Thesis, Brigham Young University, Provo, UT (2007)

[8] P.R. Murray. *Flow-Induced Responses of Normal, Bowed, and Augmented Synthetic Vocal Fold Models.* MS Thesis, Brigham Young University, Provo, UT (2011)

[9] P.R. Murray, S.L. Thomson, "Vibratory responses of synthetic, self-oscillating vocal fold models," *J. Acoust. Soc. Am.* (in review)

[10] *ADINA-F Theory and Modeling Guide Volume III: ADINA CFD & FSI.* ADINA R&D, Inc. (2010)

[11] S.L. Smith, S.L. Thomson, "Effect of inferior surface angle on the self-oscillation of a computational vocal fold model," *J. Acoust. Soc. Am.* (in press)

[12] I.R. Titze *Principles of Voice Production*, 2nd ed., National Center for Voice and Speech, Iowa City, IA, pp. 15-19, 205-207 (2000)

[13] M. Döllinger, D.A. Berry, "Visualization and quantification of the medial surface dynamics of an excised human vocal fold during phonation," *J. Voice* 20(3), 401-413 (2006)